Desalination and Water Treatment
www.deswater.com

doi: 10.1080/19443994.2015.1071684

57 (2016) 15495–15502
July

Taylor & Francis
Taylor & Francis Group

Nano-TiO_2-loaded activated carbon fiber composite for photodegradation of a textile dye

S. Tamilselvi[a,*], M. Asaithambi[a], P. Sivakumar[b]

[a]*Department of Chemistry, Erode Arts and Science College, Erode, TN 638009, India, Tel. +91 9842716561; email: s.tamilselvieac@gmail.com (S. Tamilselvi), Tel. +91 9842739526; email: asai4u@gmail.com (M. Asaithambi)*
[b]*Department of Chemistry, AA Govt Arts College, Namakkal, TN 637002, India, Tel. +91 9865366488; email: shivagobi@yahoo.com*

Received 14 September 2014; Accepted 5 July 2015

ABSTRACT

An activated carbon fiber (ASC) synthesized from silk cotton fiber had been converted into a photocatalyst by loading nano-titanium dioxide (TiO_2) [in anatase and rutile form] onto ASC. This novel photocatalyst (ASC-TiO_2) was found to be active in UV and visible region of electromagnetic spectrum, and tested for its effectiveness in the removal of organic pollutants from industrial wastewater and effluents. In this study, heterogeneous photocatalytic decomposition of methylene blue (MB)—predominantly a textile dyestuff, using the catalyst —ASC-TiO_2 had been found to be effective owing to the decomposition of organic pollutants into various harmless simple compounds like CO_2 and H_2O. Further studies were also conducted to optimize the operating conditions of this treatment by keeping initial dye concentration, catalyst load, and pH values as the causative variables. The results indicated that the catalyst was effective in alkaline medium and enhanced photodegradation of MB by ASC-TiO_2 was well explained by pseudo-first-order kinetics.

Keywords: Methylene blue; Silk cotton fiber; Adsorption; Photocatalysis and titanium dioxide

1. Introduction

Environmental pollution is unabated owing to the burgeoning human population and the consequential growth of synthetic production by the industrial sector to meet the ever increasing human needs. Among the various forms of pollution, water pollution created immediate and irreparable damages to flora and fauna. Industry categories such as textile-processing, paper, leather, and plastic discharged large amount of pollutants into the environment, especially into the water bodies. Presence of even trace amount of dyestuff causes severe water pollution owing to the non-biodegradable and carcinogenic nature of dye molecules. Presence of dye molecules in water bodies diminished the photosynthesis and thereby the primary production was also suppressed.

In order to overcome these environmental issues, it is essential to treat the industrial wastewater before discharging them into the water bodies. Many technologies were in vogue for the treatment of dye bearing wastewater such as adsorption, oxidation, reduction, electrochemical, and membrane filtration. However, these techniques have some limitations in one way or the other. Most of these methods are non-destructive and produced lot of harmful byproducts that were again difficult to dispose. These techniques transfer the dye molecule from one phase to another

*Corresponding author.

phase without degrading the pollutants completely, and incineration of these byproducts also produced toxic volatile compounds. Oxidation is one of the most widely employed safer technology for the effluent treatment purposes [1,2] and disposing of the harmless waste byproducts.

Recently, many developments have been made in the heterogeneous photocatalytic decomposition of dyes. Semiconductor photocatalysts like TiO_2, ZnO, ZnS, and CdS were successfully deployed for the decomposition of large organic molecules and dyestuff. The electronic structure of these photocatalysts makes them to act as good sensitizers for light-induced redox processes owing to their filled valence band and empty conduction band [3–6]. The photocatalytic decomposition of organic molecules shall be converted into simple harmless byproducts.

The photocatalytic activity of nano-TiO_2 is dependent on the size, morphology, and crystal structure. Semiconductor TiO_2 is an efficient photocatalyst under solar irradiation [7–10]. Carbon doped with TiO_2 is found to have excellent photocatalytic property under solar irradiation [11,12]. Though the mechanism of enhancement of photocatalytic activity of TiO_2 by carbon doping is not clear, many researchers are still working toward the development of carbon-doped TiO_2 photocatalyst. Mesoporous carbon-doped TiO_2 [12] and C-TiO_2 nanocomposites [13] are demonstrated for their excellent photocatalytic activity. The photocatalytic activity of TiO_2 is further improved by incorporation of light-harvesting mesoporous channels into mesoporous titania framework [14,15]. In this research work, nano-TiO_2 is synthesized over mesoporous activated carbon fiber prepared from silk cotton fiber (ASC). The structural characteristics and photocatalytic efficiency of ASC-TiO_2 composite under UV and visible light were also evaluated.

2. Experimental

2.1. Preparation of ASC-TiO_2 composite

All the chemicals were of analytical-grade (analytical reagents) purchased from Sigma–Aldrich, India, and were used without any further purification. Ten milliliters of titanium isopropoxide was added dropwise into a solution containing 35 ml of ethanol, 5 ml of double-distilled water, and 1 g of ASC with constant stirring. After the complete addition of all the reagents, the contents were stirred with magnetic stirrer for 4 h. During this period, the titanium isopropoxide underwent hydrolysis and the hydroxide accumulated onto the surface of ASC. Then the contents of the flask were filtered using Whatman No. 40 filter paper and calcined in muffle furnace at 400°C for 1 h. The TiO_2-coated ASC (ASC-TiO_2) was removed from muffle furnace after cooling it to room temperature and stored in a tight lid container for further photocatalysis of dye solutions.

2.2. Preparation of dye solution

Cationic dye, methylene blue (MB), with a molecular formula ($C_{16}H_{18}ClN_3S{\cdot}2H_2O$) M.W: 319, C.I No. 52,015, and λ_{max}: 665 nm, (E. Merck, India) was chosen as the adsorbate. A stock solution containing 1,000 mg of the dye per liter was prepared by dissolving appropriate amount of dye (based on percentage purity) in double-distilled water. This was used to prepare the adsorbate solution of appropriate dilutions as required by the experiment. The structure of MB is shown in Fig. 1.

2.3. Photocatalytic decomposition setup

The photocatalytic decomposition of dye solution was carried out in an annular type photoreactor, which had 16 reaction cells around the central lamp. High-pressure mercury vapor lamp (160 W, 210–240 V Philips, India make) was used as a light source at the central axis that can supply UV radiation with a wavelength of $\lambda \geq 365$ nm. The reaction cells were made of Pyrex tubes with a capacity of 110 ml. Another similar reactor made up of tungsten filament lamp at the central axis that was surrounded by 16 reaction cells made up of borosilicate glass was used for the photocatalysis under visible region. The contents present in the reaction cells are continuously stirred with magnetic stirrer during irradiation. The schematic arrangement of the photoreactor is shown in Fig. 2.

2.4. Measurement of photocatalytic activity

A known quantity of ASC-TiO_2 catalyst was added to 100 ml of MB solution of specified concentration in the sampling tube. The reaction temperature was maintained at 30 ± 3°C (room temperature) for all the

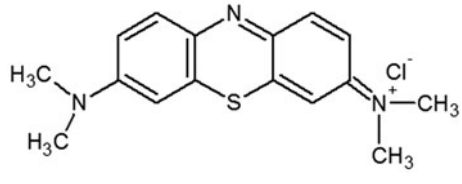

Fig. 1. Structure of MB dye.

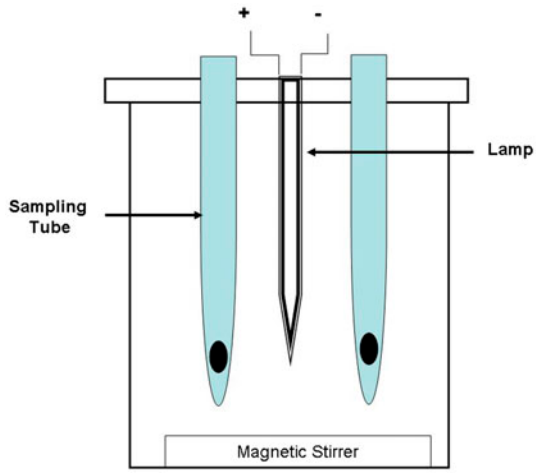

Fig. 2. Schematic diagram of the photoreactor.

experiments. The system was irradiated with a light source. After a specified time interval, the sample tube was removed from the slot, centrifuged at 5,000 rpm for 5 min using universal make centrifuge. The final concentration of dye solution was estimated by measuring the absorbance at the λ_{max} of the respective dye using UV–vis spectrometer (Elico make, model: BL-192). In order to alter the pH value, the pH of the solution was adjusted using dil. HNO_3 and NaOH. The suspension was stirred in dark for 80 min before irradiation. This time duration was determined based on the initial adsorption studies for the attainment of an equilibrated adsorption.

2.5. Characterization studies

The scanning electron microscope (SEM) images were observed using QUANTA 250 FEG field emission scanning electron microscope (FESEM). The X-ray diffraction (XRD) patterns were derived using X-ray diffractometer with Cu Kα radiation, operated at 40 kV and 30 mA. The N_2 adsorption–desorption isotherms of ASC-TiO_2 were measured at 77 K using N_2 gas sorption analyzer (Nova 1000, Quantachrome Corporation). The samples were degassed at 200˚C for 12 h before measurement. The surface area of ASC-TiO_2 composites was measured using BET isotherm model and the pore volume was calculated using BJH method.

3. Results and discussion

3.1. Characteristics of ASC-TiO_2 composite

The FESEM images of ASC fiber (Fig. 3(a) and (b)) showed a smooth surface with a diameter range of 1–5 μm before loading with titanium dioxide (TiO_2). The titania crystals were uniformly distributed in the surface ASC without much of aggregation. The surface functionalities of the ASC may hold the TiO_2 without any aggregation. The TiO_2 grown on the surface of ASC appeared to have strong interactions that led to the formation of new hybrid materials for the photocatalysis applications [16]. Fig. 4 shows the XRD pattern of ASC, pure TiO_2 and ASC-TiO_2 composite. The broad peak of ASC located between 20˚ and 30˚ was attributed to the amorphous carbon structure. The peak locations for TiO_2 were cited from the Joint Committee on Powder Diffraction Standards (JCPDS) database. The peaks located at 25˚–26˚ corresponded to the (1 0 1) plane of the anatase phase (JCPDS 21-1272). The peaks located at 38˚, 48˚ corresponded to the (1 1 2), (2 0 0) plane of anatase. The peaks located at 54˚ and 56˚, respectively, corresponded to the (2 1 1) and (2 2 0) planes of rutile phase. The location of (1 0 1) was found to be suppressed in ASC-TiO_2 composite, suggesting the surface strain and lattice distortion induced by the incorporation of carbon.

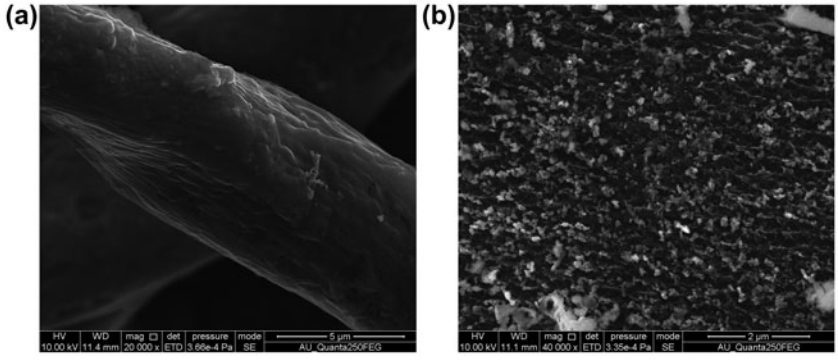

Fig. 3. (a) FESEM image of ASC and (b) FESEM image of ASC-TiO_2.

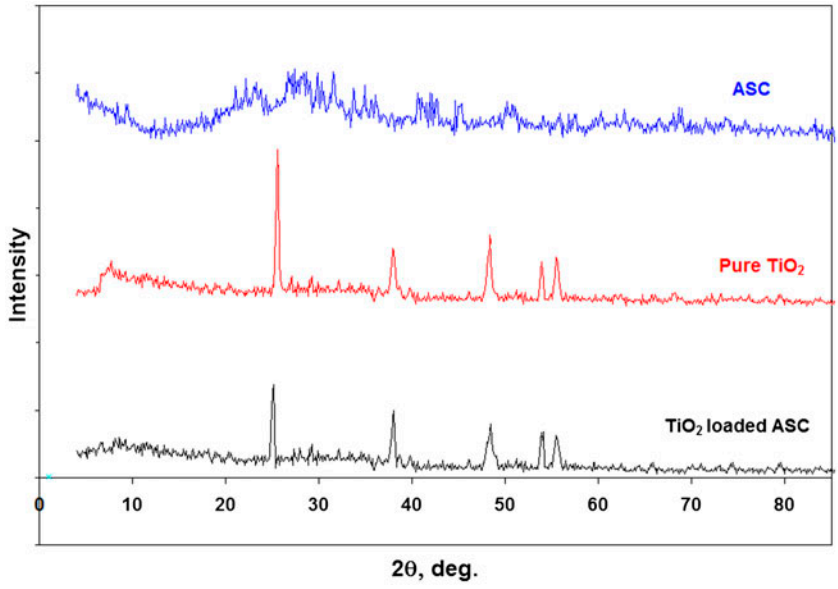

Fig. 4. XRD of ASC, TiO_2, and ASC-TiO_2 composite.

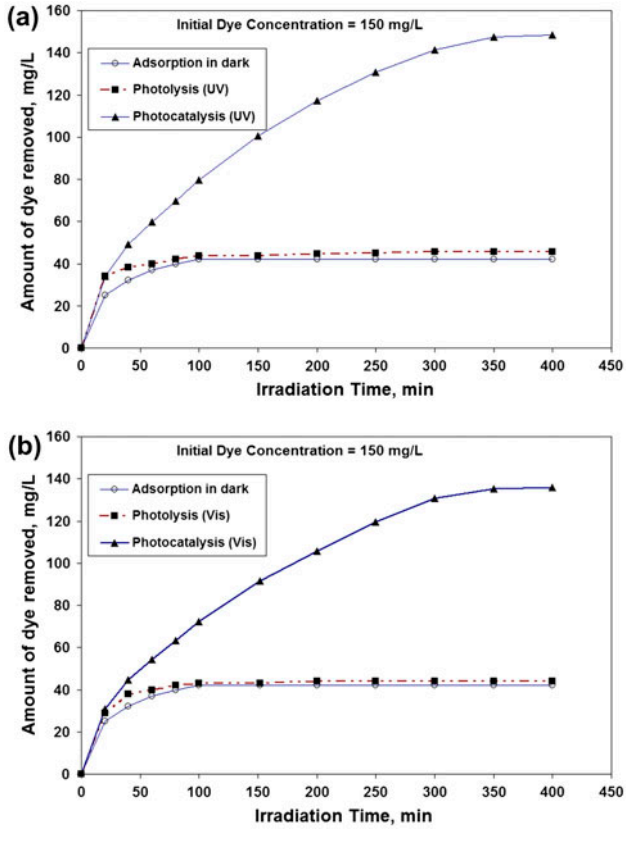

Fig. 5. (a) Effect of UV radiation on the degradation of MB and (b) effect of solar radiation on the degradation of MB.

The pore size distribution studies indicated a narrow range for ASC-TiO_2 composite, which implied good homogeneity of the pore. The ASC-TiO_2 composite had a surface area (S_{BET}) of 101.2 m^2/g, pore volume of 0.1044 cm^3/g, and pore diameter of 31.02 Å.

3.2. *Adsorption of MB by ASC-TiO_2 composite*

As the ASC-TiO_2 composite may have some adsorption capacity toward the MB dye molecule, it is essential to subtract the adsorption capacity of

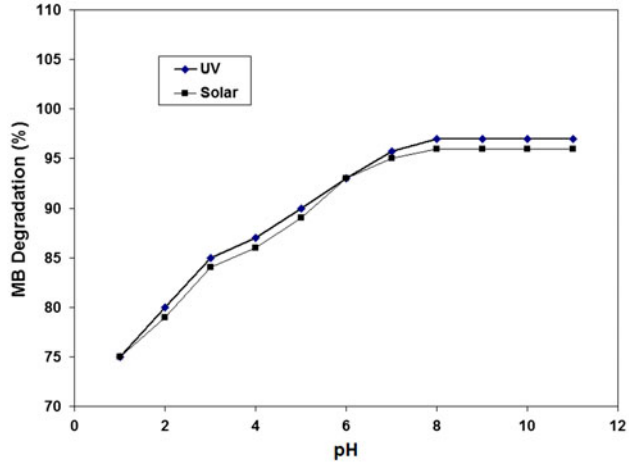

Fig. 6. Effect of pH on the degradation of MB.

composite to have a clear picture about the photocatalytic behavior of the prepared composite. The rate of change of adsorption with respect to time is shown in Fig. 5(a) and (b) at various initial dye concentrations. As seen from the Fig. 5(a) and (b), the adsorption was rapid during the beginning and it slowly decreased and finally reached equilibrium at 60 min. The amount of dye adsorbed per gram of adsorbent increased with an increase in initial dye concentration. When compared with the adsorption capacity of pure ASC, the ASC-TiO_2 composite showed poor adsorption. Since some of the active sites and pores were blocked by the presence of nano-TiO_2, which ultimately suppressed the adsorption capacity of ASC-TiO_2. For all the range of concentrations, the adsorption of MB onto ASC-TiO_2 composite showed Langmuir kind of isotherm (Type I isotherm).

3.3. Effect of pH on MB degradation

Solution pH is one of the most important environmental factors influencing the rate of photocatalytic decomposition of organic molecules [17]. During the treatment of dyeing industrial wastewater, the solution played a significant role. The discoloration of MB at a pH range of 2–11 is shown in Fig. 6. The percentage discoloration increased while increasing the pH. In particular, effective discoloration was achieved at basic pH. The zero point charge of ASC-TiO_2 composite is 6.8, which signified that the surface of the catalyst was positive when the pH was below 6.8 and it became negative when the solution pH exceeded 6.8. In the basic medium, the negatively charged ASC-TiO_2 composite attracted the cations and repelled the anions. As the MB dye is basic dye that exist as $[MB]^+$ and Cl^-. The $[MB]^+$ cations are attracted toward the negatively charged ASC-TiO_2 surface and enhanced the photocatalytic decoloration. At basic pH, more OH^- ions in the solution shall combine with the holes present on the ASC-TiO_2 surface and produce more and more OH^- radicals [18]. As the hydroxyl ions are dominant oxidizing species in the photocatalytic process, the photocatalytic decomposition of MB is observed to be high in alkaline medium [17].

In the acidic medium, the presence of Cl^- ions in the dye molecule may reduce the activity of ASC-TiO_2. Citing the following three reasons reported in the literature that the role of Cl^- ions on the decomposition rate of organic molecules is quite negative [19].

(1) At low pH (<5), the catalyst exists predominantly as $TiOH^+$ and TiOH. The negatively charged chloride ions are attached on the surface of catalyst, and ultimately minimize several active sites that cause poor degradation [20].
(2) The catalytic activity decreases owing to the poor formation of $OH^\cdot$ radicals. The reason suggested for this phenomenon is that the Cl^- acts as electron scavengers competing with molecular oxygen. Thereby the formation of super oxide followed by $OH^\cdot$ formation is prevented [21,22].
(3) The third possible reason is that the free radicals are needed in high concentrations to have an efficient photocatalytic decomposition of dye molecules [23]. Consumption of free radicals by Cl^- through some additional reactions reduces the rate of photodecomposition.

3.4. Effect of catalyst load

It was the first and foremost objective to optimize the amount of catalyst required for the effective oxidative degradation of MB dye by ASC-TiO_2. The experiment was carried out with a catalyst loading of 5–50 mg for 100 ml of dye solution of specified concentration at the natural pH of dye solution. For the optimization of catalyst loading, the contents were left for 5 h and the final concentration of the dye solution was analyzed spectrophotometrically after removing the catalyst by centrifugation. The variation of MB degradation under UV and visible region as a function of catalyst dosage is shown in Fig. 7. The amount of dye degradation increased on increasing the catalyst load from 5 to 20 mg and further increased in the catalyst loading did not show any improvement in the photodegradation of MB dye. The photodegradation of dye molecules decreased when the catalyst load

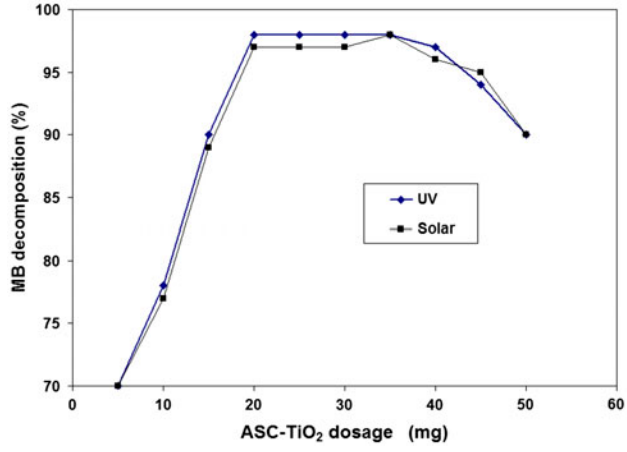

Fig. 7. Effect of catalyst dosage on the degradation of MB.

increased above 40 mg. This was due to the fact that the high concentration of catalyst prevents the effective photoabsorption and there by reduced the photodegradation. Therefore, a 20-mg catalyst load was fixed as the optimum loading for further photocatalytic degradation studies. The optimal concentration of catalyst depended on many factors like working conditions, surface area of the catalyst, and wavelength of the incident radiation [24,25].

3.5. Kinetic model to predict the rate constant for the photodegradation

The rates of photocatalytic degradation of organic molecules are independent of the concentration of hydroxyl ion concentration [26]. Therefore, the experimental data were analyzed using the following pseudo-first-order kinetic expression.

$$\ln C_t = -k_1 t + \ln C_0 \quad (1)$$

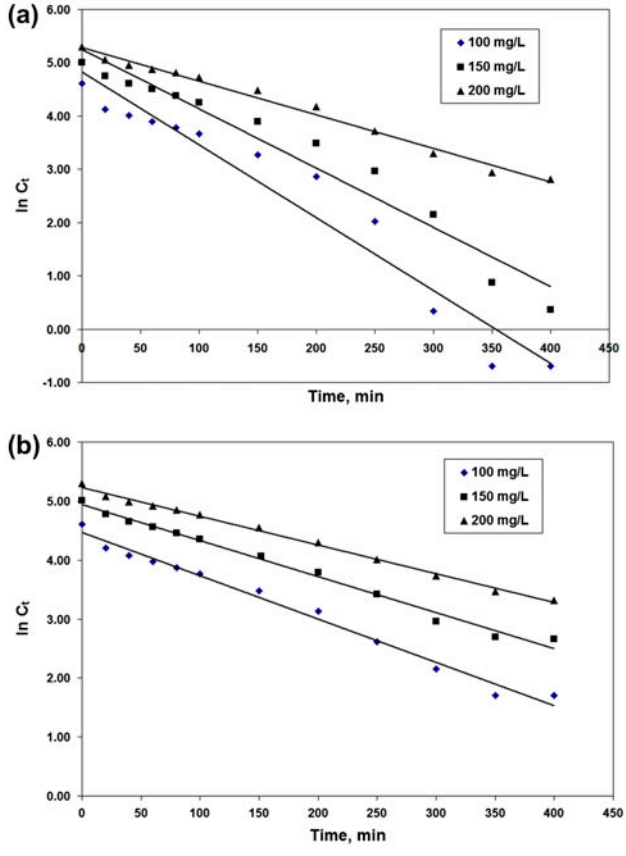

Fig. 8. (a) Pseudo-first-order plot of MB degradation under UV irradiation and (b) pseudo-first-order plot of MB degradation under solar irradiation.

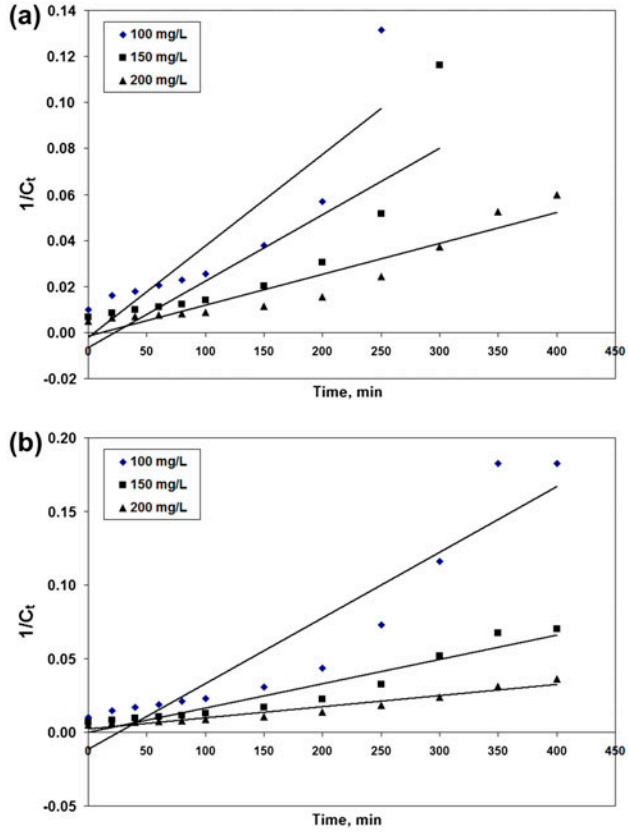

Fig. 9. (a) Pseudo-second-order plot of MB degradation under UV irradiation and (b) pseudo-second-order plot of MB degradation under solar irradiation.

where C_0 is the initial concentration of MB dye (mg/L), C_t is the concentration of MB at time t (mg/L), and k_1 is the pseudo-first-order rate constant (min^{-1}). The pseudo-first-order rate constant was determined from the slope of the plot $\ln C_t$ vs. t as shown in Fig. 8(a) and (b).

The pseudo-second-order kinetic model can be expressed as:

$$1/C_t = k_2 t + 1/C_0 \quad (2)$$

where k_2 is the pseudo-second-order rate constant and it was determined from the slope of the plot $1/C_t$ vs. t as shown in Fig. 9(a) and (b). The results of the kinetic studies are presented in Table 1. The results indicated that the pseudo-first-order rate constant decreased from 3.155×10^{-2} to 1.451×10^{-2} under UV irradiation and it decreased from 1.681×10^{-2} to 1.128×10^{-2} under solar irradiation on increasing the initial dye concentration from 100 to 200 mg/L. As the initial dye concentration increased, the effective light penetration was prevented through scattering of photons by the

Table 1
Results of the photodegradation kinetics of MB by ASC-TiO_2

Initial dye concentration (mg/L)	$k_1 \times 10^{-2}$	r^2	$k_2 \times 10^{-5}$	r^2
UV irradiation				
100	3.155	0.9431	7.62	0.7856
150	2.556	0.9535	1.41	0.7500
200	1.451	0.9886	0.67	0.8974
Solar irradiation				
100	1.681	0.9859	7.62	0.885
150	1.589	0.9903	0.63	0.926
200	1.128	0.9955	0.67	0.9424

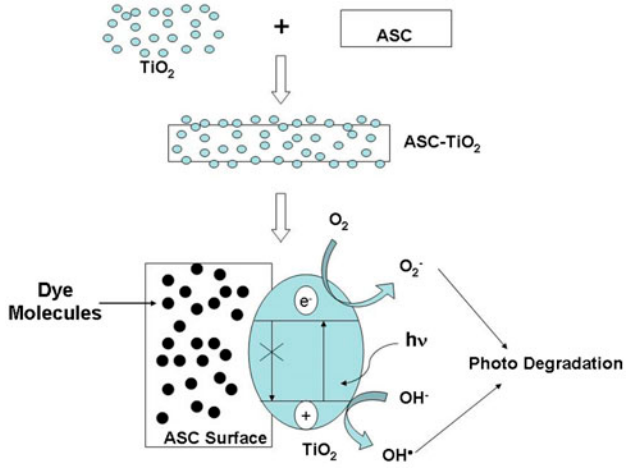

Fig. 10. Mechanism of MB degradation by ASC-TiO_2.

dye molecules that resulted in reduction of first-order rate constant. The kinetic data applied to pseudo-second-order kinetic model. The results indicated a poor fitness of the data to pseudo-second-order model owing to the very low correlation coefficient. The photocatalytic decomposition of MB by ASC-TiO_2 composite followed pseudo-first-order kinetics both under the UV and solar irradiation, with a good correlation coefficient.

3.6. Mechanism of photodegradation

The photodegradation of MB dye was improved by the ASC-TiO_2 composite. During the growth of titania over the surface of ASC, the aromatic network present on the surface prevented the agglomeration of titania and thereby nanosized titania was deposited on the surface of ASC [16]. The presence of rutile along with anatase form of titania enhanced the photodegradation. The carbon surface trapped electron–hole pair generated by the titania and thereby prevented the electron and hole recombination (Fig. 10). The hole generated the $OH^{\bullet}$ radicals and the electron generated O_2^- that were essential species for the photodegradation of organic dye molecule into some simple byproducts like CO_2 and H_2O.

4. Conclusion

The titania grown on the surface of activated ASC had nanosized TiO_2 in anatase and rutile form. The surface of ASC prevented the agglomeration that resulted in the formation of nanosized TiO_2. The ASC-TiO_2 composite was a very active catalyst in UV as well as in solar irradiation. The surface of ASC prevented the electron–hole recombination and thereby the deactivation of TiO_2 was prevented. The FESEM and XRD results proved the nano-TiO_2 deposition over ASC. The decomposition of MB was dependent on the solution pH value as well as the dosage of the catalyst. The MB degradation by ASC-TiO_2 followed pseudo-first-order kinetics with high correlation coefficient under UV and solar irradiations. The ASC-TiO_2 composite is thus a promising catalyst for the degradation of organic dyes under UV as well as solar irradiations.

References

[1] T. Fujitani, J. Nakamura, The chemical modification seen in the Cu/ZnO methanol synthesis catalysts, Appl. Catal., A Gen. 191 (2000) 111–129.
[2] J. Qin, Q. Zhang, K.T. Chuang, Catalytic wet oxidation of p-chlorophenol over supported noble metal catalysts, Appl. Catal., B Environ. 29 (2001) 115–123.
[3] S. Sakthivel, S.U. Geissen, D.W. Bahnemann, V. Murugesan, A. Vogelpohl, Enhancement of photocatalytic activity by semiconductor heterojunctions: α-Fe_2O_3, WO_3 and CdS deposited on ZnO, J. Photochem. Photobiol., A 148 (2002) 283–293.

[4] J. Araña, A.P. Alonso, J.M.D. Rodríguez, G. Colón, J.A. Navío, J.P. Peña, FTIR study of photocatalytic degradation of 2-propanol in gas phase with different TiO_2 catalysts, Appl. Catal., B Enivron. 89 (2009) 204–213.
[5] E. Rego, J. Marto, P.S. Marcos, J.A. Labrincha, Decolouration of Orange II solutions by TiO_2 and ZnO active layers screen printed on ceramic tiles under sunlight irradiation, Appl. Catal., A Gen. 355 (2009) 109–114.
[6] T. He, H. Ma, Z. Zhou, W. Xu, F. Ren, Z. Shi, Preparation of ZnS–Fluoropolymer nanocomposites and its photocatalytic degradation of methylene blue, J. Polym. Degrad. Stab. 94 (2009) 2251–2256.
[7] Y. Liu, X. Chen, J. Li, C. Burda, Photocatalytic degradation of azo dyes by nitrogen-doped TiO_2 nanocatalysts, Chemosphere 61 (2005) 11–18.
[8] T. Ohno, M. Akiyoshi, T. Umebayashi, K. Asai, T. Mitsui, M. Matsumura, Preparation of S-doped TiO_2 photocatalysts and their photocatalytic activities under visible light, Appl. Catal., A Gen. 265 (2004) 115–121.
[9] Z.B. Wu, F. Dong, W.R. Zhao, H.Q. Wang, Y. Liu, B.H. Guan, The fabrication and characterization of novel carbon doped TiO_2 nanotubes, nanowires and nanorods with high visible light photocatalytic activity, Nanotechnology 20 (2009) 235701–235709.
[10] Y.Z. Li, D.S. Hwang, N.H. Lee, S.J. Kim, Synthesis and characterization of carbon-doped titania as an artificial solar light sensitive photocatalyst, Chem. Phys. Lett. 404 (2005) 25–29.
[11] Q. Xiao, J. Zhang, C. Xiao, Z.C. Si, X.K. Tan, Solar photocatalytic degradation of methylene blue in carbon-doped TiO_2 nanoparticles suspension, Sol. Energy 82 (2008) 706–713.
[12] W.J. Ren, Z.H. Ai, F.L. Jia, L.Z. Zhang, X.X. Fan, Z.G. Zou, Low temperature preparation and visible light photocatalytic activity of mesoporous carbon-doped crystalline TiO_2, Appl. Catal., B Environ. 69 (2007) 138–144.
[13] R.L. Liu, Y.J. Ren, Y.F. Shi, F. Zhang, L.J. Zhang, B. Tu, D.Y. Zhao, Controlled synthesis of ordered mesoporous C−TiO_2 nanocomposites with crystalline titania frameworks from organic−inorganic−amphiphilic coassembly, Chem. Mater. 20 (2008) 1140–1146.
[14] G.S. Shao, T.Y. Ma, X.J. Zhang, T.Z. Ren, Z.Y. Yuan, Phosphorus and nitrogen co-doped titania photocatalysts with a hierarchical meso-/macroporous structure, J. Mater. Sci. 44 (2009) 6754–6763.
[15] X. Wang, J.C. Yu, C. Ho, Y. Hou, X. Fu, Photocatalytic activity of a hierarchically macro/mesoporous titania, Langmuir 21 (2005) 2552–2559.
[16] C.H. Kim, B.H. Kim, K.S. Yang, TiO_2 nanoparticles loaded on graphene/carbon composite nanofibers by electrospinning for increased photocatalysis, Carbon 50 (2012) 2472–2481.
[17] P. Velusamy, S. Pitchaimuthu, S. Rajalakshmi, N. Kannan, Modification of the photocatalytic activity of TiO_2 by β-Cyclodextrin in decoloration of ethyl violet dye, J. Adv. Res. 5 (2014) 19–25.
[18] S. Kaneco, M.A. Rahman, T. Suzuki, H. Katsumata, K. Ohta, Optimization of solar photocatalytic degradation conditions of bisphenol A in water using titanium dioxide, J. Photochem. Photobiol., A 163 (2004) 419–424.
[19] G. Alhakimi, S. Gebril, L.H. Studnicki, Comparative photocatalytic degradation using natural and artificial UV light of 4-chlorophenol as a representative compound in refinery wastewater, J. Photochem. Photobiol., A 157 (2003) 103–109.
[20] K. Wang, Y.H. Hsieh, M.Y. Chou, C.Y. Chang, Photocatalytic degradation of 2-chloro and 2-nitrophenol by titanium dioxide suspensions in aqueous solution, Appl. Catal., B 21 (1999) 1–8.
[21] V. Augugliaro, L. Palmisano, M. Schiavello, A. Sclafani, Photocatalytic degradation of nitrophenols in aqueous titanium dioxide dispersion, Appl. Catal., B 69 (1991) 323–340.
[22] J.M. Tseng, C.P. Huang, Removal of chlorophenols from water by photocatalytic oxidation, Water Sci. Technol. 23 (1991) 377–387.
[23] M. Abdullah, G.K. Low, R.W. Matthews, Effects of common inorganic anions on rates of photocatalytic oxidation of organic carbon over illuminated titanium dioxide, J. Phys. Chem. 94 (1990) 6820–6825.
[24] D. Chen, A.K. Ray, Photocatalytic kinetics of phenol and its derivatives over UV irradiated TiO_2, Appl. Catal., B Environ. 23 (1999) 143–157.
[25] C. Zhu, L. Wang, L. Kong, X. Yang, L. Wang, S. Zheng, F. Chen, F. MaiZhi, H. Zong, Photocatalytic degradation of AZO dyes by supported TiO_2 + UV in aqueous solution, Chemosphere 41 (2000) 303–309.
[26] N. Guettai, H. Ait Amar, Photocatalytic oxidation of methyl orange in presence of titanium dioxide in aqueous suspension. Part I: Parametric study, Desalination 185 (2005) 427–437.